Electronic Supplementary Material (ESI) for Physical Chemistry Chemical Physics.

Supplementary information

Molecular dynamics study of the interactions between a hydrophilic polymer brush on graphene and amino acid side chain analogues in water

Takuma Yagasaki* and Nobuyuki Matubayasi*

Division of Chemical Engineering, Graduate School of Engineering Science, Osaka University, Toyonaka 560-8531, Japan

t.yagasaki@gmail.com
nobuyuki@cheng.es.osaka-u.ac.jp

Pattern of grafting sites

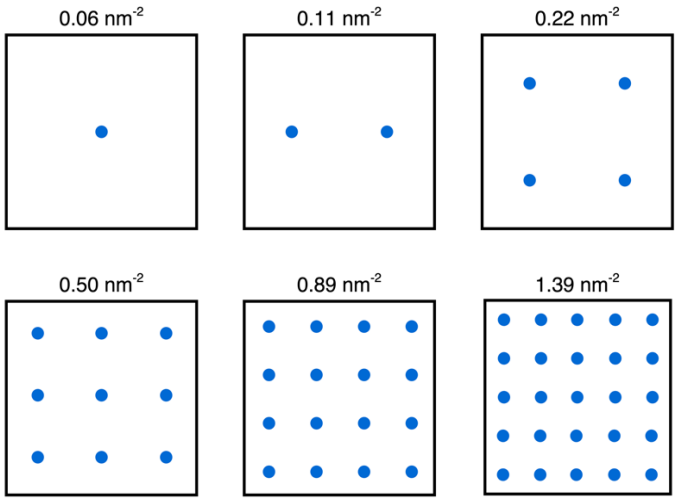

Fig. S1 Pattern of grafting sites at each grafting density.

Similarity between small and large systems

Fig. S2 schematically shows a 2D model of Sofia *et al.*[1] In this model, the grafting sites are placed in a regular square arrangement with a spacing of L. Each blue circle represents the region of a polymer chain projected onto the solid surface. The radius of this region is approximated by R_g^{iso}. There is an open space where a solute molecule can adsorb directly on the solid surface when L is larger than $2R_g^{iso}$ (panel (a)). The solute can adsorb on the solid surface even in the brush regime, $L/(2R_g^{iso}) \leq 1$, if its diameter, d_p, is smaller than $2^{1/2}L - 2R_g^{iso}$ (panel (b)). When $2^{1/2}L = 2R_g^{iso}$, the surface is fully covered by the polymer chains with no open space available for direct adsorption (panel (c)). If the interactions between the solute and the polymer chains are repulsive, the amount of solute adsorbed on the surface is dependent on the ratio, $f = (2^{1/2}L - 2R_g^{iso})/d_p$, and the interaction between the solute and the solid surface. The ratio, f, can be the same for a small particle and a large protein (the f value of a small particle and short chains is close to that of a large particle and long chains for a given L/d_p). Because we examine sufficiently wide ranges of grafting density and degree of polymerization, f covers the regime of the wide space for direct adsorption (panel (a)) to that of no open space (panel (c)). Thus, our simulations are expected to reproduce the experimental σ dependence of the amount of adsorption qualitatively.

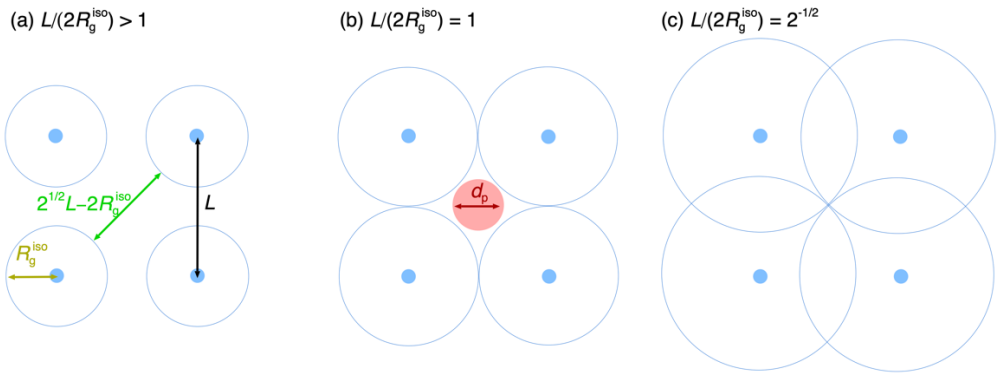

Fig. S2 Schematic of the 2D model of Sofia *et al*. The grafting sites, shown by the blue dots, are placed in a regular square arrangement with a spacing of L. Each blue circle represents the region of a polymer chain projected onto the solid surface. The radius of this region is R_g^{iso}. The red sphere shows a solute particle with a diameter of d_p.

The interactions between the solute and the polymer chains may be attractive. The binding free energy is determined by the balance between the attractive interaction and the repulsive interaction, both of which increase with the solute size. Gu *et al*. investigated the size dependence of the binding free energy of attractive solutes to polymer brushes using coarse-grained MD simulations.[2] It was shown that the attractive interaction energy is proportional to d_p^2 whereas the repulsive term due to the entropic penalty is proportional to $d_p^{4/3}$ for small solutes and to $d_p^2 + \alpha d_p^3$ for large solutes, where α is a constant. The sign of the binding free energy is almost independent of the solute size because the size dependence of the attractive interaction is not so different from that of the repulsive one, and only the magnitude of the binding free energy increases with size. In other words, whether the solute is repelled from or adsorbed onto the brush is insensitive to the solute size. This implies that the behaviors of small isobutane, propionamide, and propionate ion are likely to be qualitatively similar to those of hydrophobic, weakly hydrophilic, and strongly hydrophilic proteins, respectively.

Dynamics of polymer chains

We check the timescale of the structural relaxation of the main chains. A function $H(\tau)$ is calculated for each dihedral angle. This function is 1 when the angle is in between $2\pi/3$ and $4\pi/3$ (trans conformation) during a period of $0 < t < \tau$ and 0 otherwise. Fig. S3 shows the auto-correlation functions of H for the PHEMA brush of $n = 16$ and $\sigma = 0.50$ nm^{-2} at several temperatures. The density is kept constant at the

equilibrium value of 300 K in all the simulations. The simulation time is 100 ns and the last 50 ns is used to calculate the correlation function. The correlation function decays very quickly at 900 K. This result ensures that the polymer conformation is well randomized in the high temperature region of the annealing process to generate the initial states of the brush systems.

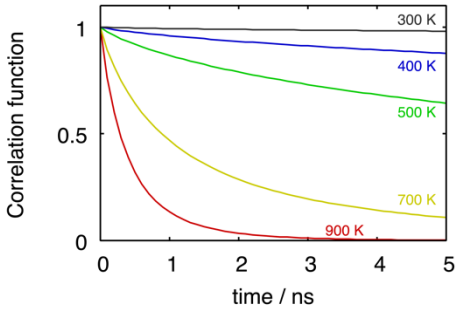

Fig. S3 Auto-correlation functions of H at several temperatures for the PHEMA brush of n = 16 and σ = 0.50 nm^{-2}.

Energetic and entropic terms in the solvation free energy

The solvation free energy of the solute at z can be expressed as

$$G(z) = -k_B T \ln\langle \exp\left(-\beta E_{\mathrm{UV}}(z)\right)\rangle_{\mathrm{cav}} - k_B T \ln\langle P_{\mathrm{cav}}(z)\rangle_{N-1} \quad \text{(S1)}$$

where β is the reciprocal temperature, E_{UV} is the solute-solvent interaction energy, and $P_{\mathrm{cav}}(z)$ is the probability of finding a cavity that can accommodate the solute.[3,4] The second term is calculated from configurations without the solute molecule, and the first term is the average over the insertion processes of the interactions with the solvent for the cavities in which the solute can be placed. This expression is known as the cavity insertion Widom method and can be used for inhomogeneous systems as well as for homogeneous systems.[5–7] The solute-solvent interaction is weak for the nonpolar solute. In this case, the solvation free energy is approximated by[8]

$$G^{\mathrm{np}}(z) = \langle E_{\mathrm{UV}}(z)\rangle_N - k_B T \ln\langle P_{\mathrm{cav}}(z)\rangle_{N-1}, \quad \text{(S2)}$$

where $\langle \cdots \rangle_N$ denotes the ensemble average with the solute. The first term disappears if the solute is a purely repulsive hard sphere. Thus, the second term can be considered as the entropic term associated with the repulsive interaction:

$$-k_B T \ln\langle P_{\mathrm{cav}}(z)\rangle_{N-1} \sim -TS_{\mathrm{UV}}(z). \quad \text{(S3)}$$

Therefore, we can identify $\langle E_{\mathrm{UV}}(z)\rangle_N$ and $-TS_{\mathrm{UV}}(z)$ of the nonpolar solute to $G_{\mathrm{vdW}}(z)$ and $G_{\mathrm{rep}}(z)$, respectively.

Simulation time and z_{aq} values

Figs. S4 and S5 show the time evolution of the amount of adsorption per unit area, Γ, which is defined in eqn (8) in the main text. Γ(t) increases rapidly at the beginning of the simulation because the diffusion of the solute molecules in water is very fast. Then the solute molecules penetrate the brush slowly. This process is absent when the graphene surface is not fully covered by the PHEMA chains. Γ seems to reach its equilibrium value within 1000 ns in all simulations. Therefore, the last 1000 ns of the trajectory is used to calculate the density profile in the main text.

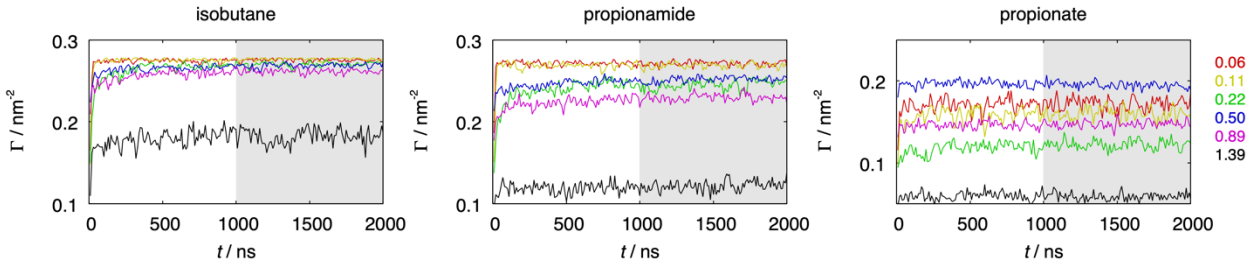

Fig. S4 Time evolution of the amount of adsorption per unit area at σ = 0.06 (red), 0.11 (yellow), 0.22 (green), 0.50 (blue), 0.89 (magenta), and 1.39 nm^{-2} (black). The degree of polymerization is 16.

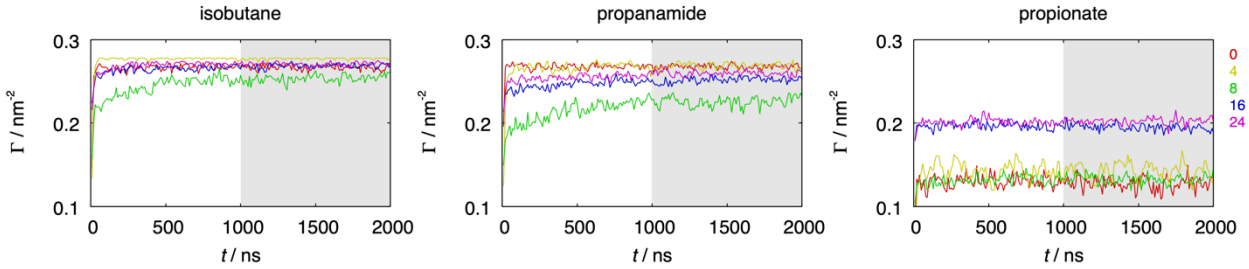

Fig. S5 Time evolution of the amount of adsorption per unit area for n = 4 (yellow), 8 (green), 16 (blue), and 24 (magenta). The grafting density is 0.50 nm^{-2}. The result for the bare graphene surface is shown by the red curve (n = 0) in each panel.

Table S1 Values of z_{aq} used to calculate Γ from eqn (8). z_{aq} is the z value at which the density of the polymer chains becomes 0.001 g cm^{-3}. z_{aq} for the bare surface is set to 0.6 nm, the same value as $z_{p\text{-}t}$. The ratio of the number of solute molecules in the bulk aqueous solution ($z > z_{aq}$) averaged over $1000 < t \leq 2000$ ns,

N_{bulk}, to the total number of the solute molecules, N_{total}, is also listed. As shown in Fig. 9a and Fig. 11, the standard error of K becomes large when this ratio is very small.

n	σ / nm^{-2}	z_{aq} / nm	N_{bulk}/N_{total}		
			isobutane	amide	ion
0	0.00	0.60	0.030	0.034	0.527
16	0.06	1.32	0.010	0.025	0.379
16	0.11	1.33	0.006	0.033	0.425
16	0.22	1.73	0.028	0.118	0.560
16	0.50	3.34	0.034	0.092	0.294
16	0.89	4.11	0.062	0.180	0.487
16	1.39	4.58	0.341	0.559	0.787
4	0.50	1.09	0.003	0.033	0.482
8	0.50	2.02	0.089	0.188	0.521
24	0.50	4.75	0.028	0.065	0.272

Temperature dependence of the radius of gyration

We perform 10 independent simulations for each n and σ. The radii of gyrations parallel and perpendicular to the normal of the graphene surface averaged over the 10 simulations are plotted against temperature in Fig. S6. Both components change smoothly with temperature and the standard error is small. The number of replicas of 10 seems to be sufficient to obtain statistically reliable results.

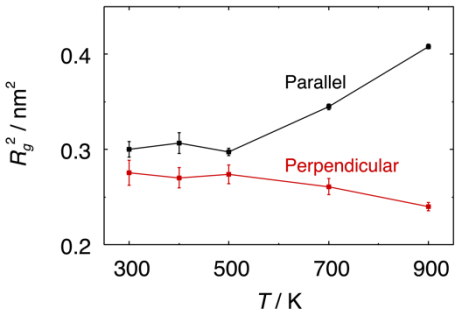

Fig. S6 Radii of gyrations parallel and perpendicular to the normal of the graphene surface for the brush of n = 16 and σ = 0.50 nm^{-2}.

Decomposition of G_{vdW}

The contribution from the vdW interaction to the Gibbs energy, $G_{vdW}(z)$, is the same as the vdW interaction energy of the fictitious nonpolar solute with all other molecules. The vdW interaction energy of a solute atom, *s*, with all atoms within a distance *R* from atom *s* is give by

$$U_s(R) = \int_0^R 4\pi r^2 \sum_a^{N_{\text{type}}} 4\varepsilon_{sa}\left(\frac{\sigma_{sa}^{12}}{r^{12}} - \frac{\sigma_{sa}^{6}}{r^{6}}\right)\rho_{sa}(r)dr, \quad \text{(S4)}$$

where ε_{sa} and σ_{sa} are the LJ energy and size parameters for a pair of atom type *s* and type *a*, $\rho_{sa}(r)$ is the radial number density function of atom *a* around atom *s*, and N_{type} is the number of atom types. Fig. S7a shows $U_s(R)$ and its components for the methyl carbon atom in isobutane located in the bulk region of the aqueous solution. The vdW interaction energy is solely due to water molecules. $U_s(R)$ decreases sharply for $0.35 < R < 0.6$ nm, indicating that water molecules in this region mainly stabilize the solute. Fig. S7b shows the result for isobutane molecules in the middle region of the PHEMA brush of $n = 16$ and $\sigma = 0.50$ nm^{-2}. The contribution from water decreases but that from PHEMA increases upon transferring the solute from the bulk to the brush. The total vdW energy is lower in the brush, indicating that the PHEMA chains stabilize the solute more efficiently than water. There are two possible mechanisms: 1) the number of LJ sites surrounding the solute is larger in the PHEMA chains than in water, and 2) the LJ interaction of each pair is stronger for the atoms in PHEMA chains than for water. The first mechanism is explained from the fact that covalent bonds in the polymer chains are much shorter than the intermolecular O-O distance in water. The second mechanism is ruled out because the LJ energy parameter of water is larger than those of all atom types in PHEMA except for one oxygen atom. Fig. S7c shows $U_s(R)$ for isobutane near the graphene surface. The solute atom is more stable near the surface than in the middle region of the brush as shown by the red curves. The contribution from graphene is comparable to that from PHEMA for the solute near the graphene surface. The graphene sheet stabilizes the solute significantly because of its high atomic density.

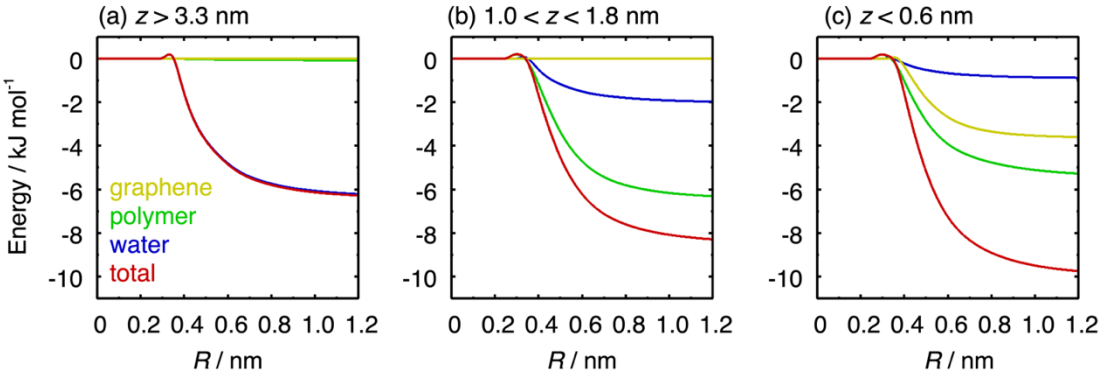

Fig. S7 vdW interaction energy between the methyl carbon atom in isobutane and LJ sites within a distance R from the methyl carbon. The degree of polymerization is 16 and the grafting density is 0.50 nm^{-2}. The yellow, green, and blue curves show the interactions with graphene, PHEMA, and water, respectively, and the red curve is the sum of them. Isobutane molecules are in the bulk aqueous region (z > 3.3 nm), in the middle region of the PHEMA brush (1.0 < z < 1.8 nm), and near the graphene surface (z < 0.6 nm) in panels (a), (b), and (c), respectively.

Figs. S8a and S8b present $U_s(R)$ for the methyl carbon of isobutane near the graphene surface for the bare surface and for the PHEMA brush of n = 16 and σ = 0.11 nm^{-2}. These two panels and Fig. S7c show that the vdW binding energy to the graphene sheet does not depend on the grafting density. The total vdW energy is lower in Fig. S8b than in Fig. S8a due to the interaction with the polymer chains.

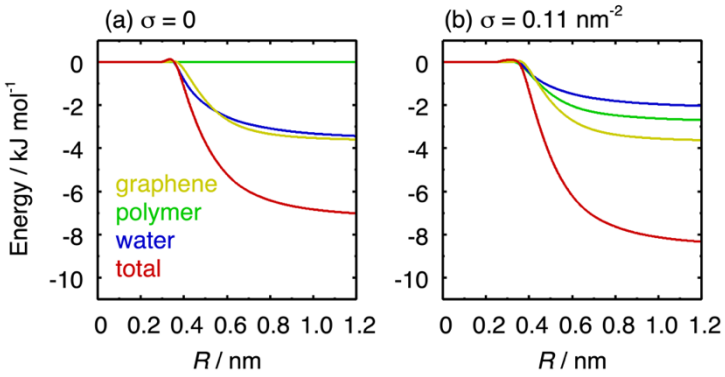

Fig. S8 vdW interaction energy between the methyl carbon atom in isobutane and LJ sites within a distance R from the methyl carbon for the solute near the graphene surface (z < 0.6 nm) at (a) σ = 0 and (b) 0.11 nm^{-2}. The degree of polymerization is 16 in panel (b). The yellow, green, and blue curves show the interactions with graphene, PHEMA, and water, respectively, and the red curve is the sum of them.

References

1 S. J. Sofia, V. Premnath and E. W. Merrill, Poly(ethylene oxide) Grafted to Silicon Surfaces: Grafting Density and Protein Adsorption, *Macromolecules*, 1998, **31**, 5059–5070.

2 C. Gu, R. D. Coalson, D. Jasnow and A. Zilman, Free Energy of Nanoparticle Binding to Multivalent Polymeric Substrates, *J. Phys. Chem. B*, 2017, **121**, 6425–6435.

3 P. Jedlovszky and M. Mezei, Calculation of the Free Energy Profile of H_2O, O_2, CO, CO_2, NO, and $CHCl_3$ in a Lipid Bilayer with a Cavity Insertion Variant of the Widom Method, *J. Am. Chem. Soc.*, 2000, **122**, 5125–5131.

4 B. Widom, Potential-Distribution Theory and the Statistical Mechanics of Fluids, *J. Phys. Chem.*, 1982, **86**, 869–872.

5 B. Widom, Structure of Interfaces from Uniformity of the Chemical Potential, *J. Stat. Phys.*, 1978, **19**, 563–574.

6 K. Shinoda, W. Shinoda and M. Mikami, Efficient Free Energy Calculation of Water Across Lipid Membranes, *J. Comput. Chem.*, 2008, **29**, 1912–1918.

7 L. B. Pártay, P. Jedlovszky, P. N. M. Hoang, S. Picaud and M. Mezei, Free-Energy Profile of Small Solute Molecules at the Free Surfaces of Water and Ice, as Determined by Cavity Insertion Widom Calculations, *J. Phys. Chem. C*, 2007, **111**, 9407–9416.

8 D. Chandler, Interfaces and the Driving Force of Hydrophobic Assembly, *Nature*, 2005, **437**, 640–647.